nature water

Article

https://doi.org/10.1038/s44221-025-00420-z

Tracking grid-level freshwater boundary exceedance along global supply chains from consumption to impact

Received: 9 July 2024

Accepted: 28 February 2025

Published online: 7 April 2025

Check for updates

A list of authors and their affiliations appears at the end of the paper

Consumption behaviours exert pressure on water resources both locally and globally through interconnected supply chains, hindering the achievement of Sustainable Development Goals 6 (Clean water and sanitation) and 12 (Responsible consumption and production). However, it is challenging to link hotspots of water depletion across spatial scales to final consumption while reflecting intersectoral competition for water. In this study, we estimated the global exceedance of regional freshwater boundaries (RFBs) due to human water withdrawal at a 5-arcmin grid scale using 2015 data, enabling the identification of hotspots across different spatial scales. To reduce uncertainty, we used average estimates from 15 global hydrological models and 5 environmental flow requirement methods. We further attributed the hotspots of exceedance to final consumption across 245 economies and 134 sectors via the multi-region input–output model EMERGING. Our refined framework revealed previously unknown connections between regional hotspots and consumption through international trade. Notably, we found that 24% of grid-level RFB exceedance (718 $km^3\ yr^{-1}$; 95% confidence interval of 659–776 $km^3\ yr^{-1}$) was outsourced through trade, with the largest flows (52 $km^3\ yr^{-1}$; 95% confidence interval of 47–56 $km^3\ yr^{-1}$) from water-stressed South and Central Asia to arid West Asia. The demand for cereals and other agricultural products dominated global consumption-based RFB exceedance (29%), while the exports of textiles and machinery and equipment exacerbated territorial exceedance in manufacturing hubs within emerging economies. Our methodology facilitates the tracing of global hotspots of water scarcity along supply chains and the assignment of responsibilities at finer scales.

Consumption in one region can have substantial impacts on water resources in other regions through global supply chains[1]. Many countries rely on imports of water-intensive products to alleviate pressure on domestic water resources[2]. A consequence of such imports is that they may shift the burden of water stress to regions that produce and export products[3–5]. For example, it has been shown that freshwater consumption in water-scarce basins in India and Pakistan is prominently driven by petroleum demand in the United States, whereas groundwater depletion in Peru has been attributed to the export of agricultural products to developed countries[4,6,7]. Hence, it is important to mitigate water impairment resulting from consumption both locally and globally, which is particularly relevant to the achievement of Sustainable Development Goals (SDGs) 6 (Clean water and sanitation) and 12 (Responsible consumption and production). To accomplish this, an essential first step is to identify the hotspots of water depletion across various spatial scales driven by the consumption of different

e-mail: xuzhao@sdu.edu.cn; xiaoxi_wang@zju.edu.cn; jing.j.meng@ucl.ac.uk; k.hubacek@rug.nl

Table 1 | Models applied to link final consumption to regional water scarcity

Indicators of regional water scarcity	Water availability models applied to evaluate regional water scarcity		Models that link final consumption to territorial water scarcity			Source
	Spatial scale	Water availability model and setting for EFR	Spatial scale	Sectoral scale	Global trade model	
Criticality ratio	National	Renewable water resources data from AQUASTAT	187 countries	26 sectors	EORA (MRIO)	Ref. 36
	Watershed	Composite Runoff V1.0 database+80% rule for EFR	27 European countries	163 sectors	EXIOBASE (MRIO)	Ref. 13
	Watershed	WaterGAP2 model	48 countries	151 sectors	EXIOBASE (MRIO)	Ref. 14
RFB	0.5° grid cell	PCR-GLOBWB model	>71 countries	26 crop classes	Process analysis	Ref. 4
	5 arcmin	Composite Runoff V1.0 database+80% rule for EFR	>20 countries	26 crop classes	Process analysis	Ref. 7
	5 arcmin	Composite Runoff V1.0 database+80% rule for EFR	174 countries	146 crops and 1 industrial sector	Process analysis	Ref. 2
	Watershed	WaterGAP2.2 model+single EFR method	>10 countries	Crop and non-crop consumption	Process analysis	Ref. 3
RFB	5 arcmin	15 global hydrological model +5 EFR methods	245 countries	134 sectors	EMERGING (MRIO)	This study

sectors along global supply chains. A modelling framework with improved sectoral and spatial resolution and reduced uncertainty is needed[8] to enable the achievement of water security through the strategic spatial layout of the economy[9].

Previous studies have acknowledged that evaluating water scarcity with high spatial resolution from a territory perspective better reflects the spatial heterogeneity of water resources, which also helps policymakers to prioritize hotspots requiring attention[10–12]. Two commonly used approaches to water scarcity assessment can show differences in local water endowment at a fine spatial resolution[4,7,13,14] (Table 1). While the criticality ratio (ratio of water use to availability) is a widely applied relative indicator[11], estimating regional freshwater boundaries (RFBs) and comparing them with a control variable (water withdrawal) provides a way to evaluate water scarcity in an absolute term[15]. Compared with a relative indicator, the RFB approach provides an appropriate form to address the strong sustainability of water resources[16] and enables the aggregation of grid-level RFB exceedance to larger spatial scales[8]. This aggregation may facilitate the identification of hotspots across different spatial scales such as urban, river basin, national and continental levels. It is worth noting that in this study we adopted the framework of 'freshwater use boundaries' proposed by Steffen et al.[15]. Recent advances have redefined both global and regional freshwater boundaries, representing them as the percentage of global or regional ice-free land area experiencing streamflow deviations from pre-industrial conditions[17,18]. Although the 'freshwater use boundaries' framework has faced criticism for its inability to fully capture the complex interactions of water with other major Earth system components[19], it is recognized as a practical and measurable approach to reflect human impacts, such as consumption and trade, on freshwater resources[8,20].

Despite its strengths, methodological improvements are still needed for the RFB approach. First, employing a single hydrological model introduces uncertainty[3,18,21] because different hydrological models yield different estimates of run-off based on their modelling characteristics, leading to diverse RFB outcomes[8,22,23]. Second, appropriate environmental flow requirement (EFR) estimation should consider diverse requirements across high-, intermediate- and low-flow seasons and use multiple methods to validate the estimates[24–26]. However, previous estimations either allocated 80% of annual blue water flows to EFRs, ignoring seasonal variations in river flows[2,7,27], or employed a single EFR method, such as the variable monthly flow (VMF) method[15], which may also introduce uncertainties[3].

Existing spatially explicit studies link national crop consumption to RFB exceedance through a process analysis, tracing exceedance at grid or watershed levels to consumption countries (Table 1). Whilst process analysis offers a detailed classification of agricultural products in international trade, multi-region input–output (MRIO) analysis encompasses all sectors of internationally traded products and their full supply chains[28–31]. As far as we know, there is no research linking the MRIO model with grid-level RFB exceedance to investigate consumption-driven RFB exceedance with improved sectoral and national detail. In summary, previous studies have been limited in at least one of the following ways (Table 1): the use of rough spatial scales, such as the national level, in production-end accounting[32,33], the introduction of uncertainties through the use of a single hydrological model for RFB estimation, the neglect of seasonal variations in EFR estimates or a focus only on agricultural products when assessing the impact of consumption on RFB exceedance.

In this study, we developed a modelling framework to assess the role of human consumption in driving RFB exceedance. We considered three major contributions. First, we estimated RFBs at a 5-arcmin grid scale using the average results from 15 global hydrological models and 5 EFR methods to reduce uncertainty (Methods). Second, we developed an inventory of water withdrawal encompassing 245 economies and 134 sectors. This inventory was aggregated from water withdrawal data collected at a 5-arcmin grid scale from the WaterGAP3 model[34] to match the national and sectoral details of EMERGING, a newly developed MRIO model[35]. The EMERGING MRIO model covers 134 sectors in 245 economies for the period 2010–2019, with over 84% classified as emerging economies. This allowed for a detailed analysis of the environmental impacts of final consumption, especially for emerging economies[35,36]. The inventory provides detailed insights into emerging and developing economies and economic sectors, which often suffer from water scarcity[12,35]. Third, we linked the consumption of various goods and services in one country to specific areas such as cities, river basins and nations where RFBs are exceeded, providing a comprehensive assessment of the impact of consumption on freshwater systems across different spatial levels. Such insights can facilitate the tracing of global water depletion hotspots along the supply chain and the assignment of responsibilities at finer scales.

Results

Sector-specific global hotspots of RFB exceedance

In 2015, global grid-scale RFB exceedance amounted to 3,021 $km^3\ yr^{-1}$ (ranging from 2,917 to 3,123 $km^3\ yr^{-1}$ with 95% confidence), equivalent to 64% of global water withdrawal (4,720 $km^3\ yr^{-1}$). The spatial distribution of exceeding grids was concentrated in 4.6% of global land area.

https://doi.org/10.1038/s44221-025-00420-z

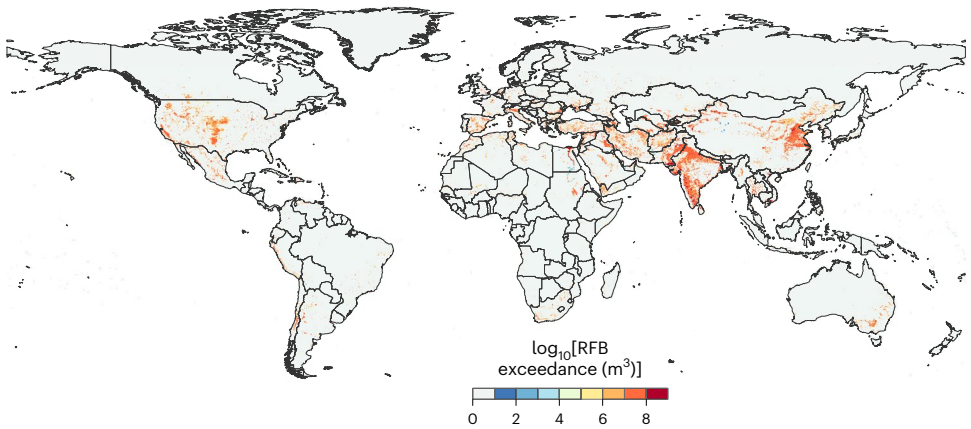

Fig. 1 | Global grid-scale RFB exceedance in 2015. Global RFB exceedance in 2015 at a 5-arcmin grid scale. The colour map is shown on the $\log_{10}$ scale.

The exceeding areas held 42% (3.1 billion) of the global population and encompassed almost all major breadbaskets or arid areas between 10° N and 50° N (Fig. 1). Hotspots with large exceedance (>100 × 10^6 m^3) accounted for just 0.18% of global land area, yet contributed 34% to global exceedance. These hotspots were located in densely populated areas such as the Beijing–Tianjin–Hebei region in China, the Mekong, Indus and Nile river deltas, as well as major urban clusters in the northeastern United States.

Attributing gridded RFB exceedance to eight major water use sectors based on each sector's share of total water withdrawals within the exceedance grid (see Methods), we found that the distribution of exceedance hotspots influenced by these sectors varied considerably. The irrigation sector, including cereals, oil seeds, edible fruits and 'other crops', collectively contributed 70% of global exceedance. Among these, 'other crops' contributed 30%, followed by oil seeds at 20%, cereals at 14% and edible fruits at 6%. The impacts of these sectors were widespread, with exceedance hotspots spanning major cereal- and oil seed-producing regions[37,38], including the North China Plain, Tarim Basin, Indus River Basin, Deccan Plateau, Tigris–Euphrates Basin, Nile River, Murray–Darling Basin in Australia, the Pacific coastal basins of the Americas and the Great Plains of the United States (Supplementary Fig. 1a–d). The largest exceedance occurred in the Nile, Ganges, Indus and Mekong river deltas. Electricity production contributed 18% of global exceedance, with hotspots scattered in areas with high electricity demand, including the eastern coast of China, the Indian Peninsula, northeastern United States and northwestern Europe (Supplementary Fig. 1f). The manufacturing sector contributed 7% of global exceedance, followed by the domestic sector, including household and services (6%). The exceedance hotspots caused by the water withdrawal of both these sectors were in densely populated areas, especially major manufacturing city clusters, including the Beijing–Tianjin–Hebei region, Yangtze and Pearl river deltas, Chengdu–Chongqing city cluster in China, Hanoi in Vietnam, Japan–Pacific Rim city cluster, New Delhi and Mumbai in India, western Europe and city clusters in eastern United States (Supplementary Fig. 1g,h). Livestock contributed only 0.2% of global exceedance (Supplementary Fig. 1e).

Aggregating grid-level RFB exceedance to the national level (adding all grids in a nation with exceedances, disregarding grids with surplus water resources), we found that the top eight economies with the highest exceedance, excluding the United States and EU28, were all emerging economies collectively contributing 58% of global exceedance (Fig. 2a and Supplementary Table 1). These countries were, in decreasing order, India, China, Pakistan, Iran, Egypt and Vietnam (for uncertainties in national exceedance, see Supplementary Tables 2 and 3). Irrigation water withdrawal was the primary contributor to RFB exceedance in these nations, accounting for 42% (Vietnam) to 99% (Afghanistan) of their respective exceedances. Electricity water withdrawal was a major contributor to exceedance in several countries, for example, 40% of RFB exceedance in the United States. Manufacturing water withdrawal played a dominant role, contributing 46% of RFB exceedance in Vietnam. When considering per capita exceedance, the top ten countries (with populations over 1 million), excluding Australia, were located in Central Asia or the Middle East and Northern Africa (MENA) region, such as Turkmenistan, Afghanistan, United Arab Emirates and Azerbaijan (Fig. 2b). The per capita exceedance of the top ten countries ranged from 1,334 to 2,794 m^3 $capita^{-1}$, equivalent to three to six times the global average volume (435 m^3 $capita^{-1}$).

National consumption responsible for global RFB exceedance

We used the MRIO approach to attribute RFB exceedance from the production perspective to national consumption. In 2015, about three-quarters (73%) of global exceedance was driven by consumption in ten major countries or regions. The countries or regions with the greatest consumer responsibility (including household withdrawal) were China (547 km^3), India (543 km^3), United States (299 km^3), European Union (EU28, including the UK in 2015, 221 km^3) and Pakistan (211 km^3). The other countries in the top ten ranking, with the exception of Russia (48 km^3), were all located in the MENA region, that is, Iran (94 km^3), Egypt (84 km^3), Iraq (58 km^3) and Saudi Arabia (57 km^3; Fig. 2c and Supplementary Table 4 for uncertainties in the national exceedance footprint). In terms of per capita consumption, countries in Central Asia and the MENA region led the rankings (for region classification, see Supplementary Table 5), that is, United Arab Emirates, Kuwait, Oman, Turkmenistan, Qatar, Saudi Arabia, Libya, Azerbaijan and Iraq, where per capita consumption exceeded 1,500 m^3 $capita^{-1}$ along the entire global supply chain (Fig. 2d). Following these countries were Australia (1,461 m^3 $capita^{-1}$), Canada (1,032 m^3 $capita^{-1}$), United States (949 m^3 $capita^{-1}$) and the EU28 (496 m^3 $capita^{-1}$). In contrast, the per capita responsibility of consumers in India and China was below the global average (435 m^3 $capita^{-1}$; Supplementary Fig. 2).

In terms of sectoral contribution, the consumption of cereals and other agricultural products accounted for 29% of RFB exceedances worldwide, followed by electricity, gas and water supply (16%), services (16%), logging and food industry (14%), and construction (6%; Fig. 3a). The consumption of agricultural sectors has a notable impact on water resources because major suppliers are located in regions heavily impacted by RFB exceedances, for example, the Indus, Ganges, Nile and Mekong river basins and the North China Plain (Supplementary Fig. 3a–d). The large impact of consumption in the logging and food industry can be attributed to their final demand for RFB-intensive products, typically cereals, oil seeds and tobacco products (Supplementary Fig. 4a,b). Notably, the livestock sector

https://doi.org/10.1038/s44221-025-00420-z

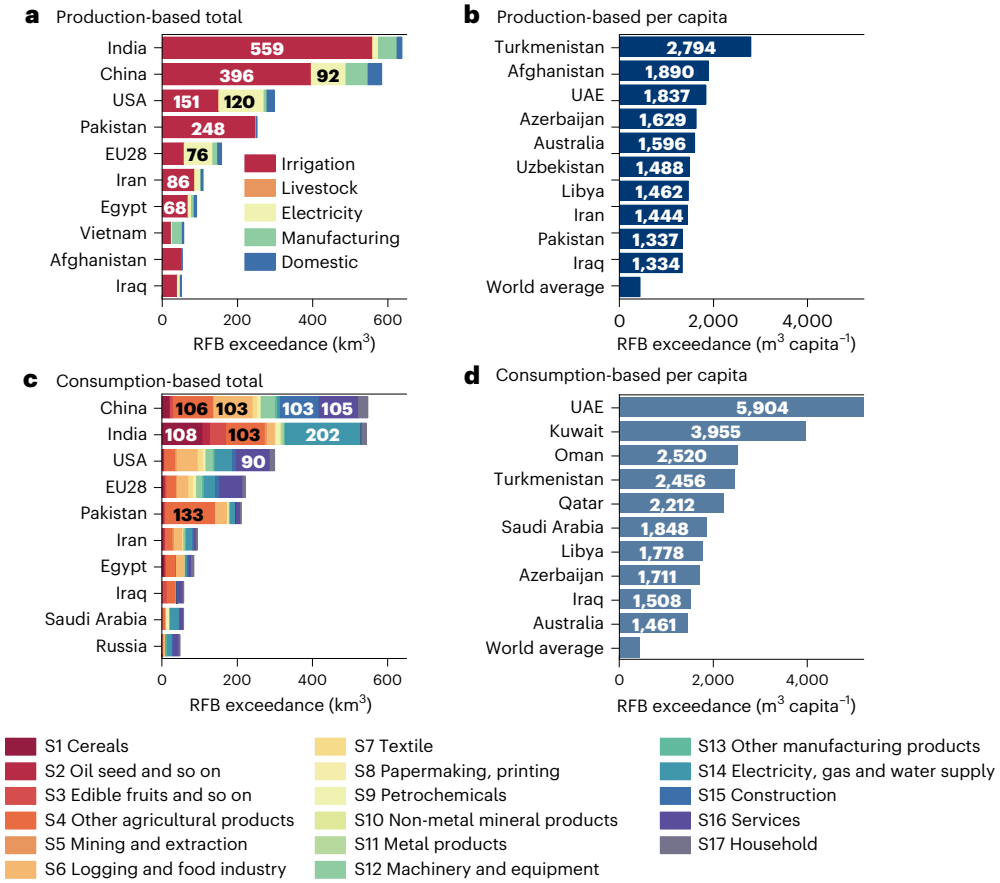

Fig. 2 | Top ten economies for RFB exceedance in 2015. a–d, Top ten economies for total production-based (**a**) and consumption-based (**c**) RFB exceedances and top 10 economies for production-based (**b**) and consumption-based (**d**) RFB exceedances per capita. The uncertainties in RFB exceedance and the RFB exceedance footprint and the 95% confidence intervals are presented in Supplementary Tables 2–4, Supplementary Fig. 5 and Supplementary Note 2. Note that the figure includes only those economies with populations over 1 million. The colour code at the bottom of the figure applies to **c** only.

(Supplementary Table 6) accounted for 12.4% of the global RFB exceedance footprint, much higher than its 0.2% contribution to global RFB exceedance from the production perspective. This discrepancy arises because consumption-based accounting encompasses not only the direct impacts of water use for livestock but also the indirect impacts throughout the supply chain, such as the use of water for producing animal feed. The impact of consumption in electricity, gas and water supply was prominent in the Ganges River, Bay of Bengal Basin, Arabian Peninsula, Western Europe and major urban clusters along the west coast and eastern United States, all of which experience high electricity demand (Supplementary Fig. 3n). Similarly, the impact of construction was evident in China, with exceedance hotspots in the Beijing–Tianjin–Hebei region, the middle and lower reaches of the Yellow River, southeastern coastal areas and the Tarim River Basin (Supplementary Fig. 3o), which have intense construction demands. In addition, the exceedance hotspots most affected by the consumption of products from the textiles and machinery and equipment sectors were located in the Mekong, Red and Indus river deltas, as well as the southeast coast of China and the Chengdu–Chongqing urban cluster (Supplementary Fig. 3g,l,m). Countries with the highest consumption of these products included the EU28, United States, MENA countries and Japan.

Outsourcing RFB exceedance through international trade

In 2015, 24% of global RFB exceedance (totalling 718.0 $km^3\ yr^{-1}$, 95% confidence interval of 659.2–775.5 $km^3\ yr^{-1}$) was embodied in internationally traded products and services. East Asia outsourced the greatest exceedance through imports of virtual water, accounting for 18.1% of global exceedance embodied in trade. This was followed by North America (15.6%), West Asia (13.4%) and Western Europe (8.6%). South and Central Asia and East Asia were the main exporters of RFB exceedance, accounting for 31.0% and 16.3%, respectively (Fig. 3b). The largest exceedance flows occurred from water-stressed South and Central Asia for the production of exports to arid West Asia, amounting to 51.8 $km^3\ yr^{-1}$. For example, as the largest exporter in South Asia, Indian exports to Saudi Arabia, Myanmar and Turkey embodied RFB exceedances of 6.3, 4.8 and 2.3 km^3, respectively. East Asia and North America are mutual primary trade partners, with large volumes of RFB exceedance. In 2015, Sino–American trade was almost balanced in terms of net exceedance: China caused 24.3 km^3 of exceedance in the United States through imports, whereas the United States caused 25.0 km^3 of exceedance in China.

We propose the outsourcing ratio to illustrate the proportion of consumption-based RFB exceedance outsourced through imports. In 2015, the regions exhibiting the highest ratios of causing exceedance elsewhere were primarily located in Europe, East Asia and Southeast Asia, including countries such as Denmark, Ireland, Sweden, United Kingdom, Singapore, Hong Kong (China) and Japan, all with ratios exceeding 80% (Supplementary Fig. 6). The hotspots of RFB exceedance driven by consumption in these countries were relatively dispersed. For example, the EU28 outsourced 60% of its consumption-based RFB exceedance, with the most affected grids dispersed in the Indus River Basin, Nile and Mekong deltas, Gulf of Thailand, Yangtze River Basin and North China Plain (Supplementary Fig. 7a). Japan outsourced 81% of its consumption-based RFB exceedance, with the grids with the largest triggered exceedance dispersed across the Korean Peninsula, the southeastern coastal areas of China, Mekong Delta, Gulf of Thailand,

https://doi.org/10.1038/s44221-025-00420-z

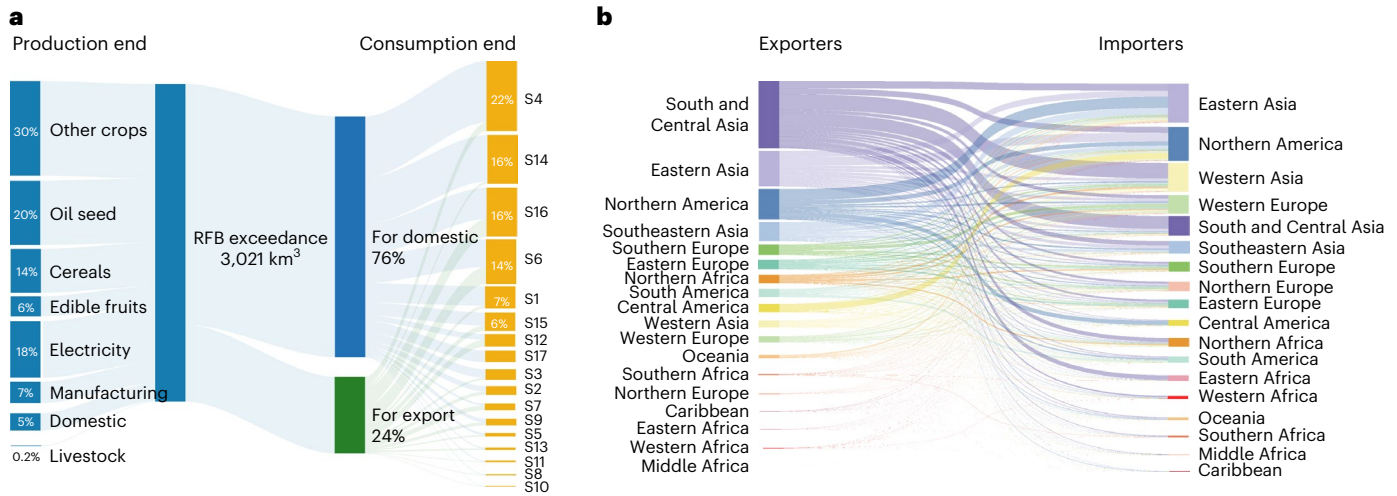

Fig. 3 | Flows of global RFB exceedance in 2015. a,**b**, Intersector flows of global RFB exceedance from production to consumption (**a**) and global RFB exceedance flows embodied in trade by region (**b**) in 2015. Labels S1–S17 are defined in the legend in Fig. 2.

Missouri Basin in the United States and the Central Valley of California (Supplementary Fig. 7b). In contrast, several countries with the largest exceedance at both the production and consumption ends had lower outsourcing ratios, including China (14%), Iran (11%), India (4%) and Pakistan (4%). The exceedance hotspots triggered by consumption in these emerging economies were concentrated within their own territories (Supplementary Fig. 7c,e,f).

International trade may foster unsustainable water use patterns, as evidenced by the MENA region. The MENA region has eased the pressure on local freshwater boundaries by importing water-intensive products and as a result it lies in the top-ranking per capita consumption-based RFB exceedance among all countries. However, this heavy reliance on external water resources may exacerbate RFB exceedance in the supplying countries. In 2015, MENA countries outsourced 16.2% of its consumption-based RFB exceedance to water-stressed South and Central Asia, particularly India, Pakistan and Iran, by importing sugars, cereals and edible fruits. This could worsen seasonal water scarcity in the Ganges, Indus and Tigris–Euphrates river basins. Moreover, trade increases vulnerability to RFB exceedance in importing regions. Beyond South and Central Asia, MENA's major import sources include China and Egypt, which, in 2015, collectively supplied about 13.7% of MENA's RFB exceedance embodied in imports. This poses potential risks to MENA's food and water security, particularly during conflicts or water crises in supplying countries[39]. In terms of net flows, we found that fewer than 15% of economies (36 out of 245) were net exporters of RFB exceedances, primarily located in South and Central Asia and West Asia. With the exception of Spain, the top ten net exporting economies with the largest RFB exceedances were all emerging economies. Conversely, among the top ten net importing economies with RFB exceedances, six were developed countries or economies (Supplementary Fig. 8a). This indicates that emerging economies dominate the net exporters (with the exception of Spain), whereas developed economies dominate net importers of RFB exceedances.

Overall, most RFB exceedance was embodied in the trade of agricultural and food products, mainly cereals, oil seeds, fruits and nuts, due to their high water intensity (Supplementary Fig. 8). The net export of cereals and oil seeds collectively accounted for 51.8% (18.1 km^3) of Afghanistan's RFB exceedance and 32.1% (179.3 km^3) of China's RFB exceedance in 2015. As the primary supplier of fruit to MENA countries, over 6.6% (7.0 km^3) of Iran's RFB exceedance was embodied in the net export of edible fruits, mainly walnuts, pistachios and citrus. Economies such as Japan, United Arab Emirates and Germany rely heavily on agricultural and food imports. In 2015, the net import of cereals and oil seeds constituted 18.4% (5.7 km^3) of United Arab Emirates' consumption-based RFB exceedance, while the net import of logging and food industry products accounted for 16.7% (6.4 km^3) of Japan's consumption-based RFB exceedance. Moreover, the export of manufactured products, textiles and services also contributes considerably to RFB exceedance, especially in emerging economies (Supplementary Fig. 8b). For example, China's net export of petrochemical products led to 7.3% (41.0 km^3) of its RFB exceedance. The net export of machinery and equipment and textile products accounted for 6.5% and 13.3% of Vietnam's RFB exceedance, respectively. Meanwhile, China, through net imports of textiles, machinery and equipment, and other manufacturing products, outsourced 44.6 km^3 of RFB exceedance to these emerging economies. This is related to industrial transfer, that is, the gradual shift of low-value-added manufacturing from China to Southeast Asian countries such as Vietnam, where production and labour costs are relatively low[40,41].

Discussion

This spatially explicit analysis that integrates detailed sectoral information is instrumental in offering insights into targeted interventions in risk hotspots. Starting from the 5-arcmin grid scale, we have identified critical grids of RFB exceedance. The grid-level results also enable the aggregation of exceedance to larger spatial scales, thereby identifying hotspots that are relevant for decision-making at those scales. Our results, based on high spatial resolution, support existing high-resolution water scarcity assessments, indicating that approximately 42% (3.1 billion) of the global population is exposed to RFB exceedance (Supplementary Table 7) and that 65% of global water withdrawals exceed their RFBs (Supplementary Table 8). Notably, our 2015 estimate closely matches the findings laid out in the United Nations World Water Development Report 2018[42], which disclosed that 3.6 billion people (47%) experienced water scarcity. Our spatially explicit analysis aligns with existing research, affirming that densely populated areas and major crop-producing regions, such as Yellow River, the Indus and Ganges river basins, and the Great Plains of the United States, exhibit the largest RFB exceedance[4,7]. In addition, our results reveal exceedance hotspots in seemingly water-abundant regions, such as urban clusters in Western Europe, the Mekong Delta in Vietnam, Gulf of Thailand, the lower Yangtze River and southeastern coastal areas of China. The sector-specific details of this study reflect the contributions of water withdrawals by different sectors to each exceedance hotspot, a facet often overlooked in previous research. For instance, the exceedance hotspots in the urban clusters of Western

Europe and the northeastern United States are mainly driven by local water demand for electricity generation (Supplementary Fig. 1 and Supplementary Table 9). These hotspots are often neglected in studies that focus solely on the irrigation sector or employ aggregated spatial scales[2–4].

Using the MRIO model, our study further attributes the territorial hotspots of RFB exceedance to final consumption along global supply chains. Notably, using the EMERGING model, due to the inclusion of more nations, we have been able to identify RFB exceedance at the consumption end for more emerging and developing economies, which was not possible in previous work. We found that exceedance hotspots in emerging economies are mostly in major cities, such as Tianjin, Shanghai, Guangzhou, Hanoi, Ho Chi Minh City and Bangkok. These cities feature world-class ports, abundant labour and a relatively strong manufacturing base[43]. The export of textile products and machinery and equipment is the main cause of their RFB exceedance, with most exports flowing to developed economies, such as Western Europe, Japan and the United States. With urbanization, the local water demand of these megacities is expected to increase. Given the trend in global industrial transfer, emerging economies, as recipients of low-value-added manufacturing, are likely to face increasingly severe RFB exceedance associated with their export production[13]. While manufacturing exports boost income and employment, they concurrently exacerbate the water crisis[44].

Addressing the above issues requires integrated actions from various stakeholders. First, producers in hotspot areas should adopt comprehensive measures towards keeping water withdrawal within their RFBs. These measures include technological advances, industrial structure upgrades and strategic adjustments to the spatial layout of the economy. Given that irrigated agriculture remains a primary contributor to RFB exceedance in many regions, the prevalent use of flood irrigation, characterized by lower water efficiency, needs to be adjusted[45]. Shifting to water-saving technologies such as drip and microsprinkler irrigation systems can effectively alleviate RFB exceedance in hotspot regions as seen, for example, in the Central Valley of California and Yellow River Basin in China[46,47]. It should be noted that we emphasize improving water efficiency within RFBs to prevent a situation where improved efficiency induces higher water withdrawal due to the rebound effect[48]. To reconcile contradictions between industrialization in emerging economies and water depletion, the scale and structure of industries should be determined according to their RFBs[43]. Governments have recognized this issue and have reflected it in policies. For example, in the 13th Five-Year Plan, the Chinese government restricts water-intensive projects in overexploited areas and grants water extraction permits in water-scarce regions to favour low-water-consuming, high-output industries[49]. Our research thus provides a scientific measurement framework for the implementation of the above policies. For regions that may struggle with initial investment costs, international cooperation is imperative to facilitate the widespread dissemination of new technologies and provide assistance in the construction of water-saving infrastructure[50,51]. Second, major importing economies should acknowledge their role in RFB exceedance and establish compensation mechanisms. For instance, adopting a water tax akin to the carbon tax could help to internalize the costs of freshwater depletion, ensuring that consumers bear responsibility for the damage they inflict on the global aquatic system and shift towards suppliers with abundant water resources and lower costs[52]. For water-scarce countries heavily reliant on imports, it is crucial to consider the freshwater boundary of the supplying countries when implementing virtual water import strategies. This would help to avoid exacerbating RFB exceedance elsewhere and reduce the risk of introducing food and water crises through imports. Adopting these strategies holds promise for mitigating human impacts on freshwater systems, thereby contributing to the achievement of SDGs 6 and 12.

This study has several limitations. First, we applied the 'freshwater use boundary' framework proposed by Steffen et al.[15], which has prompted debate for its limitations in fully representing the complex interactions between water and other major Earth system components[19]. Second, we focused solely on blue water. Other water sources, such as green water, polluted water and glacier water, are also important for both the hydrological cycle and human activities[19,53,54] but were not included in the analysis. Third, we did not consider the impact of human interactions, such as water diversion projects or water storage, on the exceedance of RFBs. Fourth, the RFB exceedance was evaluated for only one year, without accounting for temporal variations or the potential impacts of future climate change.

In addition, uncertainties in the RFB exceedance and exceedance footprint calculations exist (Supplementary Table 2). To address this, we conducted 1,000 Monte Carlo simulations, which demonstrated that the main findings are minimally impacted by uncertainties (see Supplementary Note 2 for a detailed uncertainty analysis). The global RFB exceedance footprint for 2015 is subject to an uncertainty of ±8% (95% confidence interval). For the top 50 countries with the largest exceedance footprints, accounting for over 90% of the global exceedance footprint, the uncertainty remains within ±10%. In contrast, sparsely populated countries with smaller RFB exceedance footprints, such as Somalia, exhibit higher uncertainty, ranging from −10.7% to 10.5% (Supplementary Table 4).

Methods

Estimating grid-level freshwater boundary exceedance

We measured the exceedance of RFBs through an indicator named gap to water sustainability (GWS; see the flow chart in Supplementary Fig. 9). The GWS is acquired by subtracting water withdrawal from the volume of freshwater available for human use, and define it as the RFB according to a previous study on planetary boundaries[15]. The GWS for grid cell k (GWS_k) is calculated as follows:

$$GWS_k = RFB_k - ww_k \quad (1)$$

where RFB_k is the freshwater boundary of grid cell k on an annual scale and ww_k is the annual water withdrawal. A negative value indicates RFB exceedance and a positive value indicates withdrawal within the RFB. As only exceedance was considered in this study, the GWS for was counted as 0 for positive values.

We calculated RFBs using a bottom-up approach, that is, allocating different proportions of mean monthly flows (MMFs) to meet EFRs in different flow seasons. This estimation starts at a grid cell (5 arcmin) scale and can be aggregated to obtain freshwater boundaries at different spatial scales (basin, province, country). The gridded RFB is estimated as:

$$RFB_k = \sum_{m=1:12} (MMF_k - EFR_k) \quad (2)$$

where the MMF_k is the mean monthly flow in grid cell k. For month m, MMF_k is calculated as an ensemble mean of 15 global hydrological models, namely, LPJmL, H08, WAYS, WEB-DHM-S, CLM40, DBH, JULES-B1, JULES-W1, MATSIRO, MPI-HM, ORCHIDEE, PCR-GLOBWB, SWBM, VIC and WaterGAP2.2. These models are driven by ISIMIP2a simulation protocols, which focus on historical simulations (1970–2010 on a monthly scale), enable model intercomparison on different spatial scales[55] and use daily observed climate data on a 0.5° grid cell from the Global Soil Wetness Project Phase 3 (GSWP3) dataset as input[56]. Detailed hydrological settings (for example, snowmelt and evapotranspiration schemes) have been presented previously[8]. EFRs are calculated as the ensemble mean of monthly EFRs using five state-of-the-art methods, namely Tessmann, VMF, Tennant, Q90_Q50 and Smakhtin[24]. The first two methods divide the year into high-, intermediate- and

low-flow periods and then allocate specific portions of the MMF to each. The other three methods differentiate between high- and low-flow periods[8] (Supplementary Table 10). To match the annual water withdrawal data, the monthly RFBs are aggregated on an annual scale. Uncertainties in estimating RFB exceedances using multiple hydrological models and EFR methods are discussed in Supplementary Note 2.1, which shows that the ensemble mean approach helps to reduce model uncertainties compared with the use of a single model.

Constructing the inventory for water withdrawal

The lack of sectoral information impedes environmental footprint accounting. To bridge this gap, we constructed an inventory of water withdrawal based on global gridded water withdrawal[34] to link with EMERGING, the latest and full-scale economic database (US$1 million in current price) covering 245 economies and 134 sectors[35] (Supplementary Tables 5 and 6). This involved aggregating gridded water withdrawal to a national scale and expanding the initial sectors to 134 subsectors[57] and household water withdrawal.

Global gridded water withdrawal data were collected from the WaterGAP3 model[34], which was selected for its high spatial resolution and detailed sectoral breakdown, allowing us to identify RFB exceedance hotspots by considering the spatial heterogeneity of water withdrawal across sectors. The water withdrawal data from WaterGAP3 cover five sectors: irrigation, livestock (including livestock water intake and cleaning), manufacturing, electricity (for cooling purposes in the thermoelectric power sector) and domestic (household and services). Sectoral water withdrawals were estimated using grid-level data inputs, including population, urbanization, gross value added, thermal electricity production, the actual irrigated area as a percentage of the area equipped for irrigation and livestock numbers[34,58,59]. A detailed description and validation of the sectoral water withdrawal data obtained from WaterGAP3 are provided in Supplementary Note 1.1 and Supplementary Fig. 10.

In general, the total national water withdrawal in country r includes household water withdrawal ww_r^H and water withdrawal for economic sectors i, ww_r^i:

$$\begin{aligned} ww_r &= \sum_k ww_{k\in r} \times R_{hw,r} + \sum_k ww_{k\in r} \times (1 - R_{hw,r}) \\ &= ww_r^H + ww_r^i \end{aligned} \tag{3}$$

where $\sum_k ww_{k\in r}$ is the water withdrawal in country r aggregated by water withdrawal of grid cell k belonging to country r and $R_{hw,r}$ is the proportion of household water withdrawal in country r.

For 24 agriculture-related sectors, we used the production data for 204 agricultural and 206 animal products from the FAOSTAT database[60] and the blue water footprint intensities of crop products and farm animals from the water footprint dataset[61,62] to allocate the water withdrawal of irrigation and livestock to all sectors:

$$ww_r^{ai} = ww_r^a \times \left(\frac{wi_r^{ai} \times p_r^{ai}}{\sum_i wi_r^{ai} \times p_r^{ai}} \right) \tag{4}$$

where ww_r^{ai} is the water withdrawal of agriculture-related sectors ai in country r; ww_r^a is the national total water withdrawal of irrigation/livestock, wi_r^{ai} is the blue water footprint intensity of crop products/farm animals and p_r^{ai} is the total production for 204 agricultural and 206 animal products in country r.

For the 80 sectors related to manufacturing and electricity, we first used the water inventory and the output data from EXIOBASE 3 in 2015[63] to calculate the water withdrawal intensity. Then we multiplied the water withdrawal intensity and output value of the corresponding sectors of EMERGING to obtain the raw water withdrawal volume of the 80 sectors and constrained sectoral water withdrawal by the grid-scale total national water withdrawal volume for manufacturing and electricity:

$$wi_{r\text{EXIOBASE}}^{mi} = w_{r\text{EXIOBASE}}^{mi} / x_{r\text{EXIOBASE}}^{mi} \tag{5}$$

$$ww_r^{mi} = ww_r^m \times \left(\frac{wi_{r\text{EXIOBASE}}^{mi} \times x_{r\text{EMERGING}}^{mi}}{\sum_i wi_{r\text{EXIOBASE}}^{mi} \times x_{r\text{EMERGING}}^{mi}} \right) \tag{6}$$

where $wi_{r\text{EXIOBASE}}^{mi}$ is the water withdrawal intensity of manufacturing-related sectors mi in country r; $w_{r\text{EXIOBASE}}^{mi}$ is the water withdrawal of sectors mi in country r, $x_{r\text{EXIOBASE}}^{mi}$ is the output of sectors mi from EXIOBASE 3 in country r, ww_r^{mi} is the water withdrawal of manufacturing-related sectors mi in country r; ww_r^m is the national total water withdrawal of manufacturing/electricity and $x_{r\text{EMERGING}}^{mi}$ is the output value of the corresponding sectors from EMERGING in country r.

For the 30 service sectors associated with the domestic sector, we similarly used the water inventory and output data from EXIOBASE 3rx in 2015 and the sectoral output for the corresponding sector of EMERGING to calculate the raw water withdrawal volume of the 30 service sectors. Then we calculated the urbanization rate of each economy based on its total population and the urban population from World Bank data[64], which was used to estimate the water withdrawal of the service sector in each economy[65,66] (Supplementary Table 11). Finally, the raw national water withdrawal of service sectors was constrained by the sectoral water withdrawal by the grid-scale total national water withdrawal volume for the domestic sector:

$$wi_{r\text{EXIOBASE}}^{si} = w_{r\text{EXIOBASE}}^{si} / x_{r\text{EXIOBASE}}^{si} \tag{7}$$

$$ww_r^{si} = ww_r^D \times UR_r \times \left(\frac{wi_{r\text{EXIOBASE}}^{si} \times x_{r\text{EMERGING}}^{si}}{\sum_i wi_{r\text{EXIOBASE}}^{si} \times x_{r\text{EMERGING}}^{si}} \right) \tag{8}$$

where $wi_{r\text{EXIOBASE}}^{si}$ is the water withdrawal intensity of service-related sectors si in country r; $w_{r\text{EXIOBASE}}^{si}$ is the water withdrawal of sectors si in country r, $x_{r\text{EXIOBASE}}^{si}$ is the output of sectors si from EXIOBASE 3 in country r, ww_r^{si} is the water withdrawal of service-related sectors si in country r; ww_r^D is the national total water withdrawal of the domestic sector, UR_r is the urbanization rate of country r; $wi_{r\text{EXIOBASE}}^{si}$ is the water withdrawal intensity calculated by EXIOBASE 3 and $x_{r\text{EMERGING}}^{si}$ is the output value of the corresponding sectors from EMERGING in country r.

Constructing the inventory for RFB exceedances at national level

To construct the RFB exceedance inventory, we allocated the grid-scale exceedance values to 8 main economic sectors, aggregated the grid-scale sectoral exceedances to the national scale and expanded the initial 8 sectors into 134 subsectors and household (Supplementary Fig. 9).

First, the RFB exceedance of grid k, GWS_k, was allocated across five sectors (irrigation, livestock, electricity, manufacturing and domestic (household and services)). The allocation was based on the sectoral water withdrawal ratio from WaterGAP3 (ref. 58) within each exceeding grid k. To improve the sectoral resolution of the RFB exceedance inventory, we further disaggregated the irrigation sector's RFB exceedance at the grid scale into four major water-consuming crops, namely, cereals, oil seeds, edible fruits and 'other crops'[62,67], resulting in the grid-scale exceedance for eight main sectors. This disaggregation was based on the proportion of water withdrawn by these crops within irrigation according to Mialyk et al.[67], which provides global irrigated water withdrawal for major crops at 5-arcmin resolution for 2015.

The RFB exceedances for the eight main sectors gi in grid cell k, GWS_k^{gi}, were derived as follows:

$$GWS_k^{gi} = GWS_k \times \left(\frac{ww_k^{gi}}{\sum_{gi} ww_k^{gi}} \right) \quad (9)$$

where ww_k^{gi} is the water withdrawal of one of the eight main sectors gi in the exceeding grid cell k.

Notably, the sectors of cereals, oil seeds, edible fruits and electricity align directly with the economic sectors in the EMERGING MRIO model. These four sectors together account for 88% of global RFB exceedance, maximally preserving the grid-scale characteristics of RFB exceedance.

Second, to align with the spatial and sectoral distribution of the EMERGING MRIO model, we aggregated the RFB exceedance for the eight main sectors from the grid scale to the national scale, $GWS_r^{gi} = \sum_k GWS_{k\in r}^{gi}$. For the cereals, oil seeds, edible fruits and electricity sectors, the national exceedance is simply the sum of their exceedances across all grids. For the remaining sectors, we first summed the grid-scale exceedances to obtain the national RFB exceedance for each of the four major categories. These totals were then disaggregated across the 134 sectors using national water withdrawal ratios in the EMERGING MRIO sector level (estimated from equations (4)–(7)). The sectoral mapping between the 8 main sectors and the 134 subsectors is provided in Supplementary Table 6. In addition, the national RFB exceedance for household use is derived from the domestic sector, based on the water withdrawal ratios for household and services at the national scale[66].

Linking RFB exceedances to final consumption

We used the MRIO approach[8] to calculate the RFB exceedance of country r driven by the final consumption of sector i. This included the exceedance caused by domestic consumption g_{rr} and the consumption in other countries $\sum_{r\neq s} g_{rs}$ (see Supplementary Note 1.2 for details):

$$g = g_{rr} + \sum_{r\neq s} g_{rs} = \sum_i \hat{d}_r (I - A_{rr})^{-1} \hat{y}_r + \sum_{r\neq s} \sum_i \hat{d}_r (I - A_{rr})^{-1} \hat{e}_{rs} \quad (10)$$

where $\hat{d}_r = GWS_r/x_r$ is the RFB exceedance intensity in diagonal matrix form representing the RFB exceedance of each sector per unit of output in country r; GWS_r is the RFB exceedance of country r by sector (that is, the RFB exceedance inventory estimated in the above section), which is aggregated from the grid-scale RFB exceedance, $(I - A_{rr})^{-1}$ is the Leontief inverse matrix, where I is the unit matrix and A_{rr} is the technical coefficient matrix, $\hat{y}_r$ is the final consumption of country r and $\hat{e}_{rs}$ is the export of the final products from country r to other countries.

The worldwide exceedance due to the consumption of sector i by country s, WEF_s^i, includes exceedances caused by the domestic production for domestic consumption of product i, g_{ss}^i, and exceedances caused by foreign production to meet the consumption of country s, g_{rs}^i:

$$WEF_s^i = g_{ss}^i + \sum_{r\neq s} g_{rs}^i \quad (11)$$

The exceedance footprint in country s, WEF_s, includes exceedances caused by household water withdrawal, GWS_s^H, and to meet the final consumption towards product i, WEF_s^i:

$$WEF_s = GWS_s^H + \sum_i WEF_s^i \quad (12)$$

Reporting summary

Further information on research design is available in the Nature Portfolio Reporting Summary linked to this article.

Data availability

All data required to estimate the RFB exceedance footprint are available via Zenodo at https://doi.org/10.5281/zenodo.14843563 (ref. 68). The required input for the MRIO quantification is in the Input data in code folder; the national RFB exceedance estimates and the data used for Figs. 1–3 and Supplementary Tables 1 and 3 are provided in the Output data folder. The EMERGING Multi-Regional Input-Output Table for 2015 was obtained from CEADs[35] (https://www.ceads.net/data/input_output_tables/).

Code availability

The MATLAB code developed in MATLAB R2023a used to link RFB exceedances to final consumption in this study is available in the MRIO code folder via Zenodo at https://doi.org/10.5281/zenodo.14843563 (ref. 68).

References

1. Wiedmann, T. & Lenzen, M. Environmental and social footprints of international trade. *Nat. Geosci.* **11**, 314–321 (2018).
2. Mekonnen, M. M. & Hoekstra, A. Y. Blue water footprint linked to national consumption and international trade is unsustainable. *Nat. Food* **1**, 792–800 (2020).
3. Motoshita, M., Pfister, S. & Finkbeiner, M. Regional carrying capacities of freshwater consumption—current pressure and its sources. *Environ. Sci. Technol.* **54**, 9083–9094 (2020).
4. Dalin, C., Wada, Y., Kastner, T. & Puma, M. J. Groundwater depletion embedded in international food trade. *Nature* **543**, 700–704 (2017).
5. Zhao, X. et al. Burden shifting of water quantity and quality stress from megacity Shanghai. *Water Resour. Res.* **52**, 6916–6927 (2016).
6. Holland, R. A. et al. Global impacts of energy demand on the freshwater resources of nations. *Proc. Natl Acad. Sci. USA* **112**, E6707–E6716 (2015).
7. Rosa, L., Chiarelli, D. D., Tu, C., Rulli, M. C. & D'Odorico, P. Global unsustainable virtual water flows in agricultural trade. *Environ. Res. Lett.* **14**, 114001 (2019).
8. Zhao, X. et al. Revealing trade potential for reversing regional freshwater boundary exceedance. *Environ. Sci. Technol.* https://doi.org/10.1021/acs.est.3c01699 (2023).
9. Hou, S. et al. Spatial analysis connects excess water pollution discharge, industrial production, and consumption at the sectoral level. *npj Clean Water* **5**, 4 (2022).
10. Vörösmarty, C. J. et al. Global threats to human water security and river biodiversity. *Nature* **467**, 555–561 (2010).
11. Liu, J. et al. Water scarcity assessments in the past, present and future. *Earths Future* **5**, 545–559 (2017).
12. Mekonnen, M. M. & Hoekstra, A. Y. Four billion people facing severe water scarcity. *Science* **2**, e1500323 (2016).
13. Lutter, S., Pfister, S., Giljum, S., Wieland, H. & Mutel, C. Spatially explicit assessment of water embodied in European trade: a product-level multi-regional input-output analysis. *Glob. Environ. Change* **38**, 171–182 (2016).
14. Weinzettel, J. & Pfister, S. International trade of global scarce water use in agriculture: modeling on watershed level with monthly resolution. *Ecol. Econ.* **159**, 301–311 (2019).
15. Steffen, W. et al. Planetary boundaries: guiding human development on a changing planet. *Science* **347**, 1259855 (2015).
16. Li, M., Wiedmann, T., Fang, K. & Hadjikakou, M. The role of planetary boundaries in assessing absolute environmental sustainability across scales. *Environ. Int.* **152**, 106475 (2021).
17. Richardson, K. et al. Earth beyond six of nine planetary boundaries. *Sci. Adv.* **9**, eadh2458 (2023).
18. Porkka, M. et al. Notable shifts beyond pre-industrial streamflow and soil moisture conditions transgress the planetary boundary for freshwater change. *Nat. Water* **2**, 262–273 (2024).

19. Gleeson, T. et al. The water planetary boundary: interrogation and revision. *One Earth* **2**, 223–234 (2020).
20. Tian, P. et al. Keeping the global consumption within the planetary boundaries. *Nature* **635**, 625–630 (2024).
21. Greve, P. et al. Global assessment of water challenges under uncertainty in water scarcity projections. *Nat. Sustain.* **1**, 486–494 (2018).
22. Krysanova, V. et al. How evaluation of global hydrological models can help to improve credibility of river discharge projections under climate change. *Clim. Change* **163**, 1353–1377 (2020).
23. Velázquez, J. A. et al. An ensemble approach to assess hydrological models' contribution to uncertainties in the analysis of climate change impact on water resources. *Hydrol. Earth Syst. Sci.* **17**, 565–578 (2013).
24. Pastor, A. V., Ludwig, F., Biemans, H., Hoff, H. & Kabat, P. Accounting for environmental flow requirements in global water assessments. *Hydrol. Earth Syst. Sci.* **18**, 5041–5059 (2014).
25. Virkki, V. et al. Globally widespread and increasing violations of environmental flow envelopes. *Hydrol. Earth Syst. Sci.* **26**, 3315–3336 (2022).
26. Liu, X. et al. Environmental flow requirements largely reshape global surface water scarcity assessment. *Environ. Res. Lett.* **16**, 104029 (2021).
27. Rockström, J. et al. Safe and just Earth system boundaries. *Nature* **619**, 102–111 (2023).
28. Kastner, T., Kastner, M. & Nonhebel, S. Tracing distant environmental impacts of agricultural products from a consumer perspective. *Ecol. Econ.* **70**, 1032–1040 (2011).
29. Feng, K., Chapagain, A., Suh, S., Pfister, S. & Hubacek, K. Comparison of bottom-up and top-down approaches to calculating the water footprints of nations. *Econ. Syst. Res.* **23**, 371–385 (2011).
30. Hubacek, K. & Feng, K. Comparing apples and oranges: some confusion about using and interpreting physical trade matrices versus multi-regional input–output analysis. *Land Use Policy* **50**, 194–201 (2016).
31. Feng, K., Hubacek, K. & Yu, Y. *Local Consumption and Global Environmental Impacts: Accounting, Trade-offs and Sustainability* (Routledge, 2019).
32. Feng, K., Siu, Y. L., Guan, D. & Hubacek, K. Assessing regional virtual water flows and water footprints in the Yellow River Basin, China: a consumption based approach. *Appl. Geogr.* **32**, 691–701 (2012).
33. Hubacek, K. & Sun, L. Economic and societal changes in China and their effects on water use: a scenario analysis. *J. Ind. Ecol.* **9**, 187–200 (2005).
34. Flörke, M. et al. Domestic and industrial water uses of the past 60 years as a mirror of socio-economic development: a global simulation study. *Glob. Environ. Change* **23**, 144–156 (2013).
35. Huo, J. et al. Full-scale, near real-time multi-regional input–output table for the global emerging economies (EMERGING). *J. Ind. Ecol.* **26**, 1218–1232 (2022).
36. Lenzen, M. et al. International trade of scarce water. *Ecol. Econ.* **94**, 78–85 (2013).
37. *World Food and Agriculture—FAO Statistical Yearbook 2021* (Food and Agriculture Organization of the United Nations, 2021).
38. *World Agricultural Production* (US Department of Agriculture, 2023).
39. Shumilova, O. et al. Impact of the Russia–Ukraine armed conflict on water resources and water infrastructure. *Nat. Sustain.* **6**, 578–586 (2023).
40. Yang, C. Relocating labour-intensive manufacturing firms from China to Southeast Asia: a preliminary investigation. *Bandung J. Glob. South* **3**, 3 (2016).
41. Lee, K., Qu, D. & Mao, Z. Global value chains, industrial policy, and industrial upgrading: automotive sectors in Malaysia, Thailand, and China in comparison with Korea. *Eur. J. Dev. Res.* **33**, 275–303 (2021).
42. *The United Nations World Water Development Report 2018: Nature-Based Solutions for Water* (UNESCO, 2018).
43. Paterson, W. et al. Water footprint of cities: a review and suggestions for future research. *Sustainability* **7**, 8461–8490 (2015).
44. Gu, W. et al. The asymmetric impacts of international agricultural trade on water use scarcity, inequality and inequity. *Nat. Water* **2**, 324–336 (2024).
45. Scanlon, B. R. et al. Groundwater depletion and sustainability of irrigation in the US High Plains and Central Valley. *Proc. Natl Acad. Sci. USA* **109**, 9320–9325 (2012).
46. Wada, Y., Gleeson, T. & Esnault, L. Wedge approach to water stress. *Nat. Geosci.* **7**, 615–617 (2014).
47. McDonald, R. I. et al. Urban growth, climate change, and freshwater availability. *Proc. Natl Acad. Sci. USA* **108**, 6312–6317 (2011).
48. Freire-González, J. Does water efficiency reduce water consumption? The economy-wide water rebound effect. *Water Resour. Manage.* **33**, 2191–2202 (2019).
49. *Water Resources Management and Protection in China* (Ministry of Water Resources, People's Republic of China, 2015); http://www.mwr.gov.cn/english/mainsubjects/201604/P020160406507020464665.pdf
50. He, C. et al. Future global urban water scarcity and potential solutions. *Nat. Commun.* **12**, 4667 (2021).
51. Pandey, N., de Coninck, H. & Sagar, A. D. Beyond technology transfer: innovation cooperation to advance sustainable development in developing countries. *Wiley Interdiscip. Rev. Energy Environ.* **11**, e422 (2022).
52. Sheng, J. & Webber, M. Incentive coordination for transboundary water pollution control: the case of the middle route of China's South-North water Transfer Project. *J. Hydrol.* **598**, 125705 (2021).
53. Zipper, S. C. et al. Integrating the water planetary boundary with water management from local to global scales. *Earths Future* **8**, 1–23 (2020).
54. Wang-Erlandsson, L. et al. A planetary boundary for green water. *Nat. Rev. Earth Environ.* **3**, 380–392 (2022).
55. Warszawski, L. et al. The Inter-Sectoral Impact Model Intercomparison Project (ISI–MIP): project framework. *Proc. Natl Acad. Sci. USA* **111**, 3228–3232 (2014).
56. Kim, H. *Global Soil Wetness Project Phase 3 Atmospheric Boundary Conditions (Experiment 1)* (Data Integration and Analysis System, accessed 20 June 2020); https://doi.org/10.20783/DIAS.501
57. Zhao, D. et al. Water consumption and biodiversity: responses to global emergency events. *Sci. Bull.* **69**, 2632–2646 (2024).
58. Flörke, M., Schneider, C. & McDonald, R. I. Water competition between cities and agriculture driven by climate change and urban growth. *Nat. Sustain.* **1**, 51–58 (2018).
59. Alcamo, J. et al. Global estimates of water withdrawals and availability under current and future 'business-as-usual' conditions. *Hydrol. Sci. J.* **48**, 339–348 (2003).
60. *FAOSTAT—Prodstat* (Food and Agriculture Organization of the United Nations, accessed 25 February 2016); http://faostat.fao.org/site/567/DesktopDefault.aspx#ancor
61. Mekonnen, M. M. & Hoekstra, A. Y. A global assessment of the water footprint of farm animal products. *Ecosystems* **15**, 401–415 (2012).
62. Mekonnen, M. M. & Hoekstra, A. Y. The green, blue and grey water footprint of crops and derived crop products. *Hydrol. Earth Syst. Sci.* **15**, 1577–1600 (2011).

63. Stadler, K. et al. EXIOBASE 3: developing a time series of detailed environmentally extended multi-regional input-output tables. *J. Ind. Ecol.* **22**, 502–515 (2018).
64. GNI per capita, Atlas method. ***World Bank*** http://data.worldbank.org/indicator/NY.GNP.PCAP.CD (2023).
65. Zhao, D., Hubacek, K., Feng, K., Sun, L. & Liu, J. Explaining virtual water trade: a spatial-temporal analysis of the comparative advantage of land, labor and water in China. *Water Res.* **153**, 304–314 (2019).
66. Liu, Y. *The Analysis of Water Footprint Changes and Driving Mechanism in Beijing–Tianjin–Hebei*. PhD thesis, Beijing Forestry Univ. (2016).
67. Mialyk, O. et al. Water footprints and crop water use of 175 individual crops for 1990–2019 simulated with a global crop model. *Sci. Data* **11**, 206 (2024).
68. Huo, J. et al. Tracking grid-level freshwater boundary exceedance along global supply chains from consumption to impact. *Zenodo* https://doi.org/10.5281/zenodo.14843563 (2025).

Acknowledgements

This work was supported by the National Key R&D Program of China (2023YFE0113000, X. Zhao), the National Natural Science Foundation of China (72074136, X. Zhao; 72104129, X. Zhang; 72033005, X. Zhao; 72273126, X.W.), the Major Grant in National Social Sciences of China (23VRC037, 24VHQ018, X. Zhao), the Taishan Scholar Youth Expert Program of Shandong Province (NO. tsqn202103020, X. Zhao), the China Scholarship Council PhD programme (S.H.) and the Research Grants Council of the Hong Kong Special Administrative Region, China (AoE/P-601/23-N, J.H.).

Author contributions

X. Zhao and J.M. designed the study; X.W., M.F. and D.Z. provided the data sources; S.H. and J.H. conducted the calculations; S.H., J.H., X. Zhang and M.R.T. analysed the results; X. Zhao, K.H. and Y.S. supervised and coordinated the overall research; all authors participated in the writing and revision of the paper.

Competing interests

The authors declare no competing interests.

Additional information

Supplementary information The online version contains supplementary material available at https://doi.org/10.1038/s44221-025-00420-z.

Correspondence and requests for materials should be addressed to Xu Zhao, Xiaoxi Wang, Jing Meng or Klaus Hubacek.

Peer review information *Nature Water* thanks the anonymous reviewers for their contribution to the peer review of this work.

Reprints and permissions information is available at www.nature.com/reprints.

Publisher's note Springer Nature remains neutral with regard to jurisdictional claims in published maps and institutional affiliations.

Siyu Hou[1,2,16], Jingwen Huo[3,16], Xu Zhao[1,16] ✉, Xiaoxi Wang[4,5,6] ✉, Xinxin Zhang[7], Dandan Zhao[8,9], Martin R. Tillotson[10], Yuli Shan[11,12], Martina Flörke[13], Wei Guo[14], Jing Meng[15] ✉ & Klaus Hubacek[2] ✉

[1]Institute of Blue and Green Development, Shandong University, Weihai, China. [2]Integrated Research on Energy, Environment and Society (IREES), Energy and Sustainability Research Institute Groningen (ESRIG), University of Groningen, Groningen, the Netherlands. [3]Department of Earth System Science, Ministry of Education Key Laboratory for Earth System Modeling, Institute for Global Change Studies, Tsinghua University, Beijing, China. [4]China Academy for Rural Development, Department of Agricultural Economics and Management, Zhejiang University, Hangzhou, China. [5]MAgPIE-China Research Group, Hangzhou, China. [6]Potsdam Institute for Climate Impact Research (PIK), Potsdam, Germany. [7]Business School, Shandong University, Weihai, China. [8]Department of Built Environment, School of Engineering, Aalto University, Aalto, Finland. [9]Institute of Surface-Earth System Science, School of Earth System Science, Tianjin University, Tianjin, China. [10]water@leeds, School of Civil Engineering, University of Leeds, Leeds, UK. [11]School of Geography, Earth and Environmental Sciences, University of Birmingham, Birmingham, UK. [12]Birmingham Institute for Sustainability and Climate Action, University of Birmingham, Birmingham, UK. [13]Institute of Engineering Hydrology and Water Resources Management, Ruhr University, Bochum, Germany. [14]Faculty of Architecture, Civil and Transportation Engineering, Beijing University of Technology, Beijing, China. [15]The Bartlett School of Sustainable Construction, University College London, London, UK. [16]These authors contributed equally: Siyu Hou, Jingwen Huo, Xu Zhao. ✉e-mail: xuzhao@sdu.edu.cn; xiaoxi_wang@zju.edu.cn; jing.j.meng@ucl.ac.uk; k.hubacek@rug.nl

nature portfolio

Corresponding author(s): Xu Zhao, Xiaoxi Wang, Jing Meng, Klaus Hubacek

Last updated by author(s): Feb 17, 2025

Reporting Summary

Nature Portfolio wishes to improve the reproducibility of the work that we publish. This form provides structure for consistency and transparency in reporting. For further information on Nature Portfolio policies, see our Editorial Policies and the Editorial Policy Checklist.

Statistics

For all statistical analyses, confirm that the following items are present in the figure legend, table legend, main text, or Methods section.

n/a	Confirmed
☒	☐ The exact sample size (*n*) for each experimental group/condition, given as a discrete number and unit of measurement
☒	☐ A statement on whether measurements were taken from distinct samples or whether the same sample was measured repeatedly
☒	☐ The statistical test(s) used AND whether they are one- or two-sided *Only common tests should be described solely by name; describe more complex techniques in the Methods section.*
☒	☐ A description of all covariates tested
☐	☒ A description of any assumptions or corrections, such as tests of normality and adjustment for multiple comparisons
☒	☐ A full description of the statistical parameters including central tendency (e.g. means) or other basic estimates (e.g. regression coefficient) AND variation (e.g. standard deviation) or associated estimates of uncertainty (e.g. confidence intervals)
☒	☐ For null hypothesis testing, the test statistic (e.g. *F*, *t*, *r*) with confidence intervals, effect sizes, degrees of freedom and *P* value noted *Give P values as exact values whenever suitable.*
☒	☐ For Bayesian analysis, information on the choice of priors and Markov chain Monte Carlo settings
☒	☐ For hierarchical and complex designs, identification of the appropriate level for tests and full reporting of outcomes
☒	☐ Estimates of effect sizes (e.g. Cohen's *d*, Pearson's *r*), indicating how they were calculated

Our web collection on statistics for biologists contains articles on many of the points above.

Software and code

Policy information about availability of computer code

Data collection	MATLAB R2023a
Data analysis	We use the MATLAB R2023a to run the code for Multi-Regional Input-Output (MRIO) analysis, which derives the result of RFB exceedance inventory at the country level and the RFB exceedance footprints. The input data and code have been deposited at https://doi.org/10.5281/zenodo.14843563.

For manuscripts utilizing custom algorithms or software that are central to the research but not yet described in published literature, software must be made available to editors and reviewers. We strongly encourage code deposition in a community repository (e.g. GitHub). See the Nature Portfolio guidelines for submitting code & software for further information.

Data

Policy information about availability of data

All manuscripts must include a data availability statement. This statement should provide the following information, where applicable:

- Accession codes, unique identifiers, or web links for publicly available datasets
- A description of any restrictions on data availability
- For clinical datasets or third party data, please ensure that the statement adheres to our policy

All data required to estimate the RFB exceedance footprint has been deposited on Zenodo at: https://doi.org/10.5281/zenodo.14843563. The required input for the MRIO quantification has been deposited in the file "Input data in code"; the national RFB exceedance estimates, and the data used for Figures 1-3, Tables S1

and S3 are provided in the "Output Data" file. The EMERGING Multi-Regional Input-Output Table for 2015 was obtained from CEADs35 (https://www.ceads.net/data/input_output_tables/).

Research involving human participants, their data, or biological material

Policy information about studies with human participants or human data. See also policy information about sex, gender (identity/presentation), and sexual orientation and race, ethnicity and racism.

Reporting on sex and gender	n/a
Reporting on race, ethnicity, or other socially relevant groupings	n/a
Population characteristics	n/a
Recruitment	n/a
Ethics oversight	n/a

Note that full information on the approval of the study protocol must also be provided in the manuscript.

Field-specific reporting

Please select the one below that is the best fit for your research. If you are not sure, read the appropriate sections before making your selection.

☐ Life sciences ☒ Behavioural & social sciences ☐ Ecological, evolutionary & environmental sciences

For a reference copy of the document with all sections, see nature.com/documents/nr-reporting-summary-flat.pdf

Behavioural & social sciences study design

All studies must disclose on these points even when the disclosure is negative.

Study description	We estimate the exceedance of regional freshwater boundaries (RFBs) due to human water withdrawal at a 5-arcmin grid scale using 2015 data, enabling the identification of hotspots across different spatial scales. To reduce uncertainty, we use average estimates from 15 global hydrological models and 5 environmental flow requirement methods. We further attribute the hotspots of exceedance to final consumption across 245 economies and 134 sectors via a MRIO model, EMERGING. Our refined framework reveals previously unknown connections between regional hotspots and consumption through international trade. The data used in this study are quantitative.
Research sample	A total of 245 economies were selected because the EMERGING MRIO model provides data for 245 economies. The EMERGING MRIO is an existing dataset that covers 134 sectors across these economies for the period 2010–2019, with over 84% classified as emerging economies. This comprehensive coverage enables a detailed analysis of the environmental impacts of final consumption, particularly in emerging economies. The EMERGING MRIO can be obtained from CEADs (https://www.ceads.net/data/input_output_tables/).
Sampling strategy	The selection is determined by the availability of data in the EMERGING MRIO model, which provides data for 245 economies. Since this model is an existing dataset, the study does not independently sample economies but instead relies on the predefined scope of the dataset.
Data collection	The global gridded water withdrawal data across five sectors (Irrigation, Livestock, Manufacturing, Electricity, and Domestic) was sourced from WaterGAP3 (https://doi.org/10.1016/j.gloenvcha.2012.10.018). To integrate this with EMERGING, the latest full-scale economic database covering 245 economies and 135 sectors, we constructed the inventory of water withdrawal using water withdrawal ratios from the FAOSTAT database (https://www.fao.org/faostat/en/#home). The EMERGING Multi-Regional Input-Output Table for 2015 was obtained from CEADs (https://ceads.net/user/index.php?id=1274&lang=en).The researchers did not influence or modify the underlying datasets, as all data were obtained from publicly available sources. Since the study is based on secondary data analysis, researcher blinding to experimental conditions or the study hypothesis was not applicable.
Timing	All data was collected between June, 2022 and June, 2023.
Data exclusions	No data were excluded from the analyses.
Non-participation	No participants were involved in the study.
Randomization	Since this study relies on secondary data analysis rather than experimental or survey-based data collection, randomization was not relevant or applicable. The datasets used—WaterGAP3, FAOSTAT, and EMERGING MRIO—are established, publicly available databases that comprehensively cover water withdrawal and economic activities across predefined economies and sectors.

Reporting for specific materials, systems and methods

We require information from authors about some types of materials, experimental systems and methods used in many studies. Here, indicate whether each material, system or method listed is relevant to your study. If you are not sure if a list item applies to your research, read the appropriate section before selecting a response.

Materials & experimental systems

n/a	Involved in the study
☒	☐ Antibodies
☒	☐ Eukaryotic cell lines
☒	☐ Palaeontology and archaeology
☒	☐ Animals and other organisms
☒	☐ Clinical data
☒	☐ Dual use research of concern
☒	☐ Plants

Methods

n/a	Involved in the study
☒	☐ ChIP-seq
☒	☐ Flow cytometry
☒	☐ MRI-based neuroimaging

Plants

Seed stocks	n/a
Novel plant genotypes	n/a
Authentication	n/a